

ON THE INFLUENCES OF SAND RIPPLES UPON THE SEDIMENT TRANSPORT IN OPEN CHANNELS

Tsubaki, Toichiro
Research Institute for Applied Mechanics, Kyushu University

Kawasumi, Tsuruo
Research Institute for Applied Mechanics, Kyushu University

Yasutomi, Takeshi
Research Institute for Applied Mechanics, Kyushu University

<https://hdl.handle.net/2324/7157921>

出版情報 : Reports of Research Institute for Applied Mechanics. 2 (8), pp.241-256, 1953-12. 九州大学応用力学研究所
バージョン :
権利関係 :

**ON THE INFLUENCES OF SAND RIPPLES
UPON THE SEDIMENT TRANSPORT
IN OPEN CHANNELS**

By Tōichirō TSUBAKI, Tsuruo KAWASUMI
and Takeshi YASUTOMI

The present authors have carried out through the experiments in long channels in order to study the scale of sand ripples in connexion with their influences on the character of flow and sediment transport. At first the measurements of the scale and advance velocity of the ripples are described and they are discussed relating with the hydraulic conditions of the flow. And further it is pointed out that there exists a close correlation between the equivalent roughness of the flow and the scale of the sand ripples and that the rate of transport of the sediment appreciably decreases under the equal tractive force, being influenced by the existence of the sand ripples.

1. Introduction. Our knowledge on the law of sediment transport is increasing more and more in these days in consequence of the extensive investigations which are aimed to clarify the general mechanism of the transport of the bed materials in the open channels. Nevertheless, this phenomenon being so complicated in nature, many important problems are still left behind without any satisfactory theory. In particular, one of the most troublesome features of them is the tendency of the bed to develop the surface waves. Once such waves exist the flow of the stream near the bed and the motion of the sand must be remarkably influenced by them. In fact recent studies show that their appearance is followed not only by the increase of the flow resistance but by the decrease of the rate of transport of the sediment under the equal tractive force. Thus we can suppose the significant rôle of sand ripples in practical problems of sediment. As far as the authors are informed, however, former observations of sand ripples are too fragmental to sketch their complex nature and the following question has been answered neither experimentally nor theoretically: that is, to what extent does the nature of sand ripples depend on the hydraulic conditions of the flow and the properties of the sediment? Or how does the sand ripple influence on the alluvial stream with sand transport?

In order to make some contributions to these problems the present authors planned observations in the channels of large scale with special reference to the sand ripples. In this paper their details are reproduced and

the influences of sand ripples on the sediment transport are experimentally demonstrated with the observed data of the sand ripples obtained through the systematic and quantitative measurements.

2. Method of Observation. The experiment has been performed in the artificial irrigation-channels of rectangular cross-sections which locate along the Hii River. These are built of concrete and have total lines of about 5 km; on their original concrete bed, the sands transported from the Hii River are deposited in about 30 cm thickness and move continually downstream, forming beautiful sand ripples as shown in Fig. 1. As these channels are favourable for our present purpose, the authors conducted there a few observations of the sand ripples, the flow characteristic of the stream and the rate of sediment transport in the summer of 1952. Considering the properties of bed materials as well as the hydraulic condition of the flow, four of these channels, A, B, C, and D were chosen for sake of variety, of which A and B were used for the main observations, and C and D for the supplementary ones. Incidentally the preliminary test was carried out in another channel E just one year before. Channels A, C and D are 2 m wide, B 0.8 m and E 3.8 m respectively. Channel B was appropriate for the purpose of investigating the condition near the so-called critical tractive force. All of these channels are very nearly straight over the sufficiently long distance and the flow discharge can be controlled by the sluice gates placed at the upstream end of each channels. In order

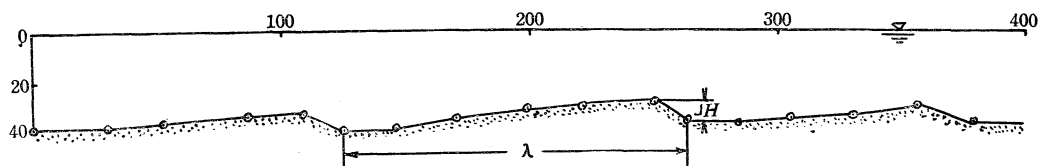


FIG. 1. Longitudinal Form of Sand Ripples.

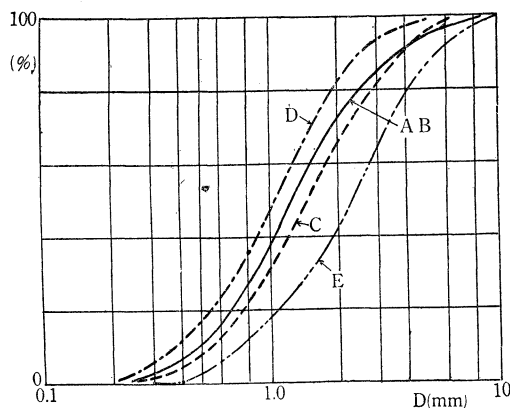


FIG. 2. Cumulative Frequency Diagram of Bed Materials.

to obtain the steady state the discharge had been kept constant during 12 hours before the measurement except few cases where the gates were adjusted 2 hours before. Fig. 2 shows the cumulative frequency diagram of the bed materials, the specific weight of which is 2.66.

(a) **Measurements of the Sand Ripple.** In reality each individual sand ripple is not uniform in its scale but has somewhat irregular size. So in the case of measurement we have to take the mean value over the considerable number of the ripples in order to find the desired quantities correspond to the hydraulic conditions of flow as a whole. In the present work the depth of water at the trough of the ripple h_T , that at the crest h_V , wave-length λ and the distance between trough and crest l were directly measured for each individual ripple, and averaging them over about 20 successive ripples, the height, $\Delta H = h_V - h_T$, wave length λ , etc. were determined. The advance velocity of the ripples u_r were evaluated from the mean displacement of each crest during the definite time interval for some 10 successive ripples. This interval was taken to be so long that the error of measurement does not exceed 5% and the ripples which deform remarkably within this interval were excluded.

The degree of fluctuation of the scales can be seen from Table 1, where the standard deviations of the measured values in channel A are tabulated with the mean values. We must say from this that the deviations are rather remarkable even in these channels of regular shape.

TABLE 1. Mean value (\bar{x}) and standard deviation (σ) of the sand ripples.

S		h_V (cm)	h_T	ΔH	λ	l	u_r (cm/sec)
1.61×10^{-3}	\bar{x}	20.9	18.6	2.27	104	3.5	0.132
	σ	0.65	0.69	0.77	35.6	1.44	0.0363
1.67×10^{-3}	\bar{x}	32.3	26.8	6.30	137	7.80	0.103
	σ	1.77	1.76	1.47	31.8	2.50	0.0182

(b) **Measurements of the Velocity.** A pitot-tube of Prandtl type (1 cm in outer diameter) and current meter of Hiroi type were used to measure the transverse velocity distribution at the center of the channel. But when the sand ripples exist, the velocity at any fixed point in the stream varies periodically with the advance of the ripples, and sometimes additive local flow due to the deformation of the ripples can be observed. Accordingly the measurements were made at the troughs, crests and middle points of several successive ripples respectively and their results were meaned. Though the accuracy of Hiroi's current meter itself is not so

sufficient for the present depth of water, it was used to find the mean value of the velocity, being properly corrected by the pitot-tube.

(c) **Measurements of the Bed Load.** If we observe carefully the motion of the individual sand grains, it is seen that they tumble down from the crest along the steep descent of the lee side of the sand ripple and the quantity of the suspended load was quite negligible in the present case. Thus the load sampler should have an intake, which is long enough to catch the moving sands, and at the same time should be large enough to receive the whole quantity of the sands contained in a full wave-length, since the rate of sand transport is never uniform at various part of the ripples. Besides it is naturally desired that the shape of the sampler is designed so as to minimize the local disturbances on both of the flow and the sediment movement. Taking these requirements into account an iron sampler

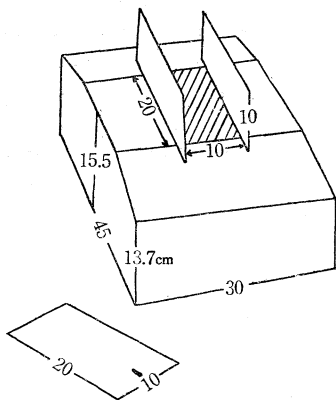


FIG. 3. Bed Load Sampler.

sampler of Fig. 3 were used. The practice of measurement is as follows: first we embed the sampler in the bed, its intake being covered, when the upper edge of the sampler should coincide with the mean depth of the trough. Since this, of course, disturbs the sediment transport to some extent we must wait several distorted samples pass by the sampler until a typical ripple for that flow comes. As its front reaches the intake, we take away the cover adjusting properly the depth of the upper edge of the sampler. The rate of transport was determined from thus sampled sediment of one wave-length. But these procedures called for considerable labours and

times, so the authors were obliged to measure at most two typical ripples for each hydraulic conditions of the flow.

The results of these measurements (a), (b) and (c) are summarized in Table 2, where the following notations are used:

$h = \frac{h^v + h_T}{2}$: arithmetic mean of the depth of the crest and that of the trough.

S : surface slope.

$u_* = \sqrt{g h S}$: shear velocity.

\bar{u} : mean velocity.

s_s : specific weight of sand in water.

D_{65} etc.: sieve size of which 65% etc. of the mixture is finer.

q : rate of transport in volume of material per unit time (1 sec), per unit width of cross-section (1 cm).

$\Psi = \frac{u_*^2}{s_s g D_{50}}$: dimensionless representation of tractive force acting on a grain.

$\Phi = \frac{q}{\sqrt{s_s g D_{50}^3}}$: dimensionless representation of rate of transport.
 λ and ΔH : wave-length and height of sand ripple.

TABLE 2. Results of observations.

h (cm)	$S \times 10^3$	u_* (cm/sec)	\bar{u} (cm/sec)	λ (cm)	ΔH (cm)	u_r (cm/sec)	q (cc/sec-cm)	$\frac{\Delta H}{h}$	$\frac{\lambda}{h}$	$\bar{v} = \frac{u_*^2}{s_s g D_{50}^3}$	$\frac{\bar{u}}{u_*}$	$\frac{k_s}{h}$	$\Phi = \frac{q}{\sqrt{s_s g D_{50}^3}}$	$\Phi' = \frac{\Delta H \cdot u_r}{2 \alpha \sqrt{s_s g D_{50}^3}}$
[Channel. A] $D_{35}=0.95, D_{50}=1.26, D_{65}=1.68$ (mm)														
15.6	1.69	5.08	58.0	120	2.85	0.126	0.162	0.182	7.69	0.126	11.40	0.132	0.0898	0.0523
18.6	1.73	5.61	—	116	2.73	0.109	0.297	0.147	6.25	0.154	—	—	0.165	0.0434
19.8	1.61	5.59	62.6	106	2.27	0.132	0.212	0.112	5.36	0.152	11.20	0.138	0.118	0.0427
24.7	1.66	6.35	69.9	131	5.35	0.092	0.249	0.216	5.29	0.196	11.00	0.149	0.138	0.0717
24.9	1.63	6.30	68.6	114	3.27	0.101	—	0.131	4.58	0.194	10.89	0.156	—	0.0452
25.7	1.61	6.36	67.0	136	4.97	0.099	0.286	0.194	5.30	0.198	10.53	0.180	0.159	0.0717
29.2	1.67	6.91	73.4	138	5.93	0.103	0.366	0.204	4.73	0.233	10.62	0.174	0.203	0.0891
34.4	1.66	7.48	75.8	150	6.68	0.089	0.383	0.194	4.36	0.273	10.13	0.211	0.212	0.0868
35.5	1.66	7.59	70.6	147	6.40	0.093	—	0.180	4.15	0.281	9.28	0.297	—	0.0868
46.7	1.66	8.72	76.5	158	8.26	0.101	0.522	0.177	3.38	0.371	8.77	0.365	0.289	0.122
[Channel. B]														
10.8	1.69	4.22	54.9	105	1.02	0.141	0.0806	0.095	9.75	0.087	13.00	0.0671	0.0448	0.0210
14.5	1.72	4.94	60.3	83	1.54	0.124	0.0669	0.107	5.74	0.119	12.22	0.0917	0.0371	0.0278
14.8	1.75	5.04	—	106	2.35	0.103	—	0.158	7.15	0.124	—	—	—	0.0353
15.7	1.65	5.04	—	93	1.65	0.092	0.105	0.105	5.92	0.124	—	—	0.0582	0.0222
17.3	1.66	5.31	61.6	91	1.95	0.096	—	0.112	5.25	0.138	11.60	0.116	—	0.0273
23.1	1.61	6.03	63.0	87	2.95	0.132	—	0.127	3.77	0.177	10.45	0.186	—	0.0567
30.7	1.64	7.02	68.4	129	7.02	0.082	—	0.229	4.20	0.241	9.74	0.247	—	0.0840
[Channel. C] $D_{35}=1.09, D_{50}=1.46, D_{65}=1.96$ (mm)														
29.5	1.37	6.30	66.1	127	5.60	0.071	0.261	0.190	4.30	0.167	10.49	0.183	0.116	0.0466
35.8	1.40	7.00	69.0	150	6.38	0.054	0.314	0.178	4.20	0.207	9.85	0.236	0.139	0.0404
35.9	1.46	7.16	74.0	134	5.40	0.078	0.433	0.151	3.74	0.216	10.34	0.195	0.192	0.0493
[Channel. D] $D_{35}=0.80, D_{50}=1.03, D_{65}=1.37$ (mm)														
30.9	0.80	4.92	53.6	106	5.08	0.052	—	0.164	3.43	0.145	10.90	0.155	—	0.0521
36.1	0.88	5.58	53.3	157	7.08	0.044	—	0.195	4.35	0.186	9.56	0.265	—	0.0614
[Channel. E]* $D_{35}=1.65, D_{50}=2.28, D_{65}=2.95$ (mm)														
10.8	1.91	4.48	—	113	0.9	0.252	—	0.084	10.5	0.054	—	—	—	0.0136
25.2	1.91	6.87	74.8	123	3.6	0.20	—	0.14	4.88	0.127	10.9	0.156	—	0.043
27.0	1.91	7.11	73.0	133	3.4	0.15	—	0.13	4.93	0.136	10.3	0.200	—	0.031
29.2	1.91	7.39	74.1	131	3.6	0.15	—	0.12	4.49	0.147	10.0	0.222	—	0.033
30.5	1.91	7.55	77.5	136	4.5	0.13	—	0.15	4.47	0.154	10.3	0.201	—	0.034
32.9	1.91	7.84	75.6	112	3.9	0.11	—	0.12	3.41	0.166	9.65	0.256	—	0.026

* This series was a preliminary test and was a little less accurate than the others.

3. On the Scale of Sand Ripple. According to the text-book of hydraulics [1] an empirical formula

$$\lambda = h \sqrt{2} \pi \frac{\bar{u}}{\sqrt{g h}}, \tag{1}$$

was early proposed by Boussinesq for the wave-length of the sand ripples. Later investigators also observed many interesting phenomena concerning the sand ripples, in the course of flume experiments on the rate of sediment transport or resistance law of the open channels with movable beds, but they seem to have not attacked the sand ripples themselves beyond the fragmental informations. Under these circumstances the first step to establish the legitimate theory of sand ripples must be to find out from the quantitative data the universal functional form, which expresses the scale of sand ripples as a function of the hydraulic characteristics and of the bed materials.

Before proceeding to this, however, let us begin with the description of the appearance of sand ripples observed in the channels A and B (their mean surface slope is 1.66×10^{-3}). When the depth of water is about 6 cm, the equilibrium of the bed is just lost; the finer grains begin to move and are sorted to form the sand ripples of about 1 m in length and a little less than 1 cm in height. As the increase in the depth, and accordingly in the tractive force, the coarser grains set in the motion in turn and the ripples grow up more and more both in length and height. During this stage the height increases more rapidly than the length, that is the "steepness" of the ripples $\Delta H/\lambda$ becomes large. At the same time it must be noted that the finer grains gather together near the crest and the coarser ones constitute the base and the trough. Each individual grain moves up along the rear side, rolling, sliding or making short hops and then tumbles down in a stratum from the crest into the vortices of the dead-water region along the steep lee side. Then the greater part of the grains are transported again to the rear of the antecedent ripple, being lifted by the local flow due to the periodic collapses of the vortices, and others are buried under the surging ripple. While these processes are continually repeated, the ripples themselves slowly advance downstream with the velocity u_r .

Considering these facts, it is naturally supposed that λ and ΔH are influenced from the following physical quantities: the gravitational acceleration g ; the specific weight of the sand in water s_s , the representative grain-diameter of the bed materials D , the dimensionless parameter of non-uniformity of the bed materials β , the kinematic viscosity of water ν , the shear velocity u_* and the scale of the existing disturbances L . Besides since the irregularity of the bed due to sand ripples produces nonuniformity of the flow, and the undulation of the free surface (especially in the experimental flume) the effects of Froude number $\bar{u}/\sqrt{g\bar{h}}$ and the scale of the standing surface waves, which can be steady in that channel, may be considered. The scale of disturbances L is assumed to be determined by those of the predominant turbulence and the standing surface waves in the channel, and hence roughly proportional to the depth of water h . Finally the functional relations

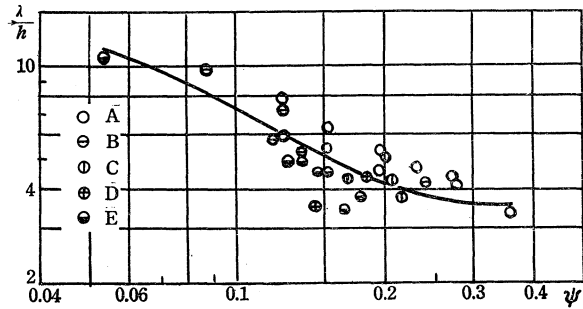
$$\frac{\lambda}{h} \text{ and } \frac{\Delta H}{h} = f\left(\frac{u_*^2}{s_s g D}, \frac{\bar{u}}{\sqrt{g\bar{h}}}, \frac{u_* D}{\nu}, \frac{h}{D}, \beta\right), \quad (2)$$

are inferred from the dimensional considerations. From this point of view the Boussinesq's formula (1) is a special case of (2), where only the effect of Froude number is taken into consideration. Comparing our experimental results with (1), we find considerable discrepancies between them qualitatively as well as quantitatively, λ/h increasing markedly even for narrow range of Froude numbers (0.3–0.6). Thus our present measurements must be analysed from another new standpoint. Of the various parameters contained in (2), β (for instance, Kramer's M can be used) is almost invariant throughout all of our tests and u_*D/ν as well as h/D may be considered to have the indirect influence through the parameter $u_*^2/s_s gD$, for $u_*D/\nu = u_*\sqrt{s_s gD} \cdot \sqrt{s_s gD^3}/\nu$ and $h/D = u_*^2/s_s gD \cdot s_s/S$. By this reason the rôles of these parameters can be disregarded here. Furthermore, because, not only the surface waves were not observed in our cases, but the Froude number was not largely varied as is mentioned above, we may suppose the predominant influence of the dimensionless tractive force $u_*^2/s_s gD$ rather than that of Froude number. So that taking in the followings the grain diameter of the 50% level of the cumulative frequency digram, or D_{50} as the representative size of the grains and denoting $\Psi = u_*^2/s_s gD_{50}$, we can expect that our present data are likely to be expressed in the form

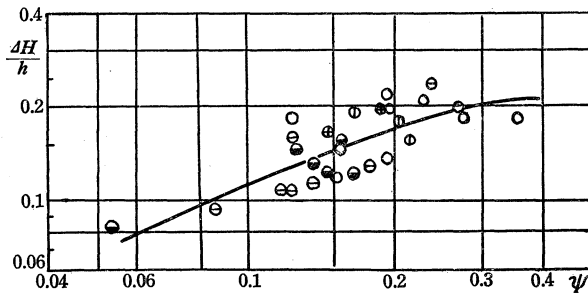
$$\frac{\lambda}{h} \quad \text{and} \quad \frac{\Delta H}{h} = f(\Psi). \quad (2')$$

Thus the observed values of λ/h are plotted in Fig. 4(a), $\Delta H/h$ in Fig. 4(b) and the steepness $\Delta H/\lambda$ in Fig. 4(c) respectively against Ψ . λ/h decreases with the increase of Ψ from about 10 at the critical tractive force Ψ_c , whereas $\Delta H/h$ increases with Ψ , and hence $\Delta H/\lambda$ increases, too. However, these changes do not take place indefinitely, but have a tendency to converge to the final states. In fact both of λ/h and $\Delta H/\lambda$ seem to become nearly constant for $\Psi = 0.2-0.4$. Particularly it is worthwhile to note that the values of λ/h scatter between 3-5, having the mean value of about 4 in this Ψ -range. Professor Kurihara, in his previous paper [2], conjectured that the scale of the predominant turbulence in the channel is probably about 4 times the depth of water. This statement is in accordance with the present result, which will offer a significant suggestion for the physical mechanism of the sand ripples. While the gentle slope of the rear side is roughly measured by the wave steepness, the steep slope of lee side is always about 33° , irrespective of Ψ . This value is almost equal to that by S. Nagai [3], who obtained 32° for the short ripples in his flume experiment, and a little larger than the angle of repose of sand in water, being considered to be influenced by the adverse flow in the vorteces region. On the advance velocity u_r of the sand ripples, various empirical formulas have been proposed up to the present based on the observations. In all of them u_r is expressed in terms of \bar{u} , but the authors found in the tests of the channels A, B and E that when the depth of water and accordingly \bar{u} is small u_r is nevertheless appreciably large. So it seems to be inadequate to consider u_r as the function of \bar{u} only.

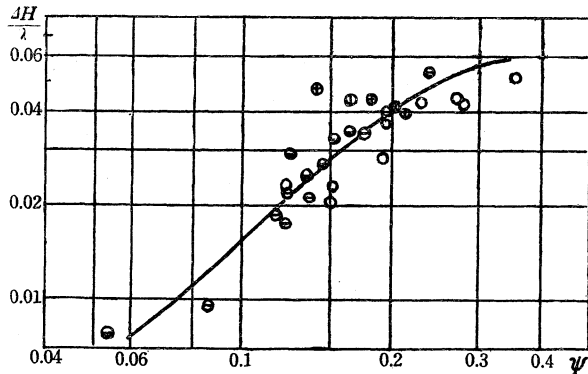
The essential feature of the movement of the sand ripples is the transport of bed materials downstream. Now approximating the shape of actual sand ripples of length λ and height ΔH by triangle, the volume of sand ripples which cross the unit width in unit time must be $\Delta H \cdot u_r / 2$ and substantial volume of sands themselves is $\Delta H \cdot u_r / 2\alpha$. From a simple test α is found to be nearly equal to 1.90.



(a) Wave Length



(b) Wave Height



(c) Wave Steepness

FIG. 4. Scales of Sand Ripples.

Introducing the non-dimensional expression $\Phi' = \Delta H \cdot u_r / 2\alpha\sqrt{s_s g D_{50}^3}$ here, it will be a function of the tractive force Ψ , too. In fact as is seen from Fig. 5 (a) we can write approximately

$$\Phi' = 0.67 \Psi^{1.5}. \tag{3}$$

On the other hand, since $\Delta H/h$ is also a function of Ψ , $hu_r / 2\alpha\sqrt{s_s g D_{50}^3}$ becomes a function of Ψ in turn. This is shown in Fig. 5 (b) where the full line can be expressed by the relation

$$\frac{hu_r}{\sqrt{g D_{50}}} = 7.03 \frac{S}{\sqrt{s_s}}. \tag{4}$$

Thus u_r is proportional to the surface slope S independently of the depth h . In conclusion it is supposed that in considerable number of natural rivers

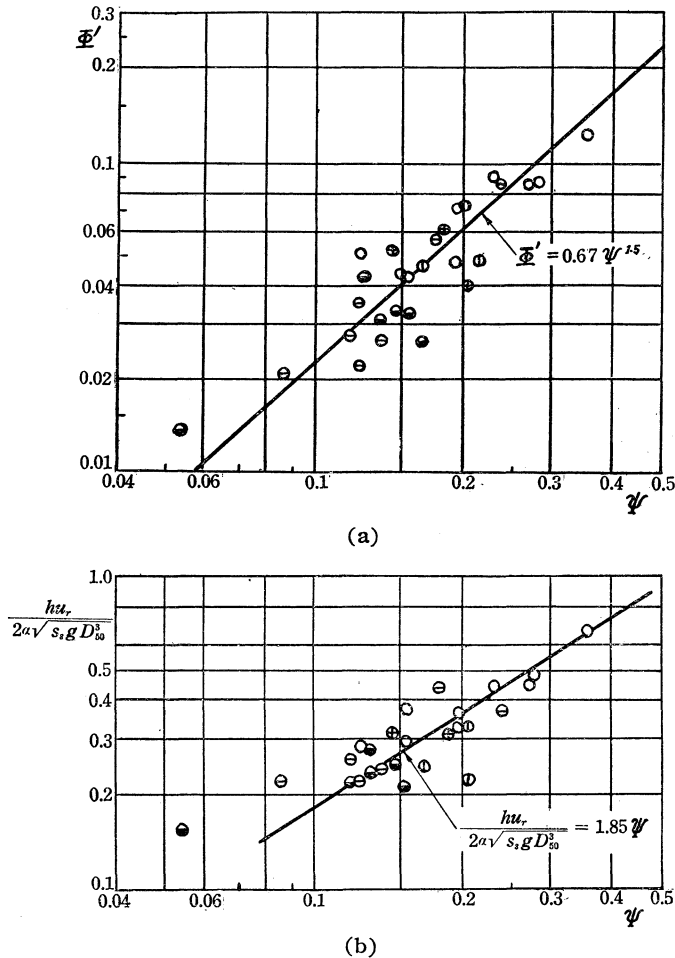


FIG. 5. Advance velocity of Sand Ripples.

in our country, the values of h/D , \bar{u}/\sqrt{gh} , u_*D/ν and β are not so much different from those in our present tests that the above analysis is able to be similarly applied to them. However for the sand ripples of small scale observed in an experimental flume, the influence of these additive parameters must be taken into consideration, and their complicated characters need further studies in future.

4. The Flow above the Sand Ripples. The remarkable increase of the flow resistance due to sand ripples has been early noticed and studied by K. Aki and S. Sato [4] in the experimental flume, or by H. A. Einstein [5] and one of the present authors [6] in the rivers with sediment transport. But all of these authors concerned the measurements of the stream velocity only without referring to the sand ripples themselves. So let us discuss this problem here based on the simultaneous observations of the ripples and the velocities. The measured values of the velocity are plotted against $\log y$ in Fig. 6, where y is the distance from the position of the average bed, that is, the origin is taken at the middle of the crest and the trough. Then it is seen the velocity profiles always obey the logarithmic law

$$\frac{u}{u_*} = 8.5 + 5.75 \log \frac{y}{k_s}. \quad (5)$$

(5) is the well established Prandtl-Kármán distribution in a circular pipe or an open channel. Here k_s has the meaning of representing the scale of the roughness of the bed and is called the "equivalent roughness of the channel." In any ordinary channel without sand ripples this scale is a constant, and so the measured points lie always on a single straight line in the $u/u_* - \log y$ diagram for given slope S , whatever the depth of water is. When the sand ripples exist, however, this straight line shifts to the right as the increase of the depth (Fig 6). In other words, the equivalent

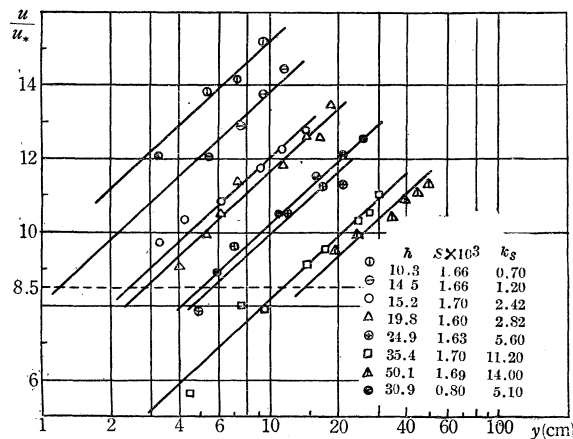


Fig. 6. Velocity Distribution of the Flow with Sand Ripples.

roughness, being prescribed by the scale of the ripples, changes with the depth of water or Ψ .

Integrating (5) and introducing the correction coefficient of Keulegan, we have for the mean velocity

$$\frac{\bar{u}}{u_*} = 6.25 + 5.75 \log \frac{h}{k_s}. \quad (6)$$

Thus the problem of the river with sediment transport is reduced to find the value of k_s for each conditions of the flow.

Now if Ψ is below the critical value, the bed materials do not move and k_s is the order of magnitude of the grain-diameter; for instance it is identified with D_{65} by H. A. Einstein [5]. Corresponding to the critical state the value of shear velocity u_{*c} is given by $u_{*c}^2/\beta s_s g D_{50} = 0.033^{1)}$ and the critical depth of water h_c becomes 6.1 cm for the channels A and B, where the mean slope of the free surface is about $S = 1.66 \times 10^{-3}$. The observed value $h_c \doteq 6$ cm agrees very well with this. Incidentally we see $(\bar{u}/u_*)_c = 15.2$ from the critical condition $\Psi_c = 0.048$ putting $\beta = 1.45$ for the present tests.

Dimensional analysis suggests us that once the sand ripples exist the equivalent roughness k_s is expressed in the form

$$\frac{k_s}{\Delta H} = f \left(\frac{\Delta H}{\lambda}, \frac{\Delta H}{D} \right),$$

where for remarkable sand ripples the direct influence of their scales becomes larger than that of the grain diameter. Again considering the fact that both of the $\Delta H/h$ and λ/h are functions of Ψ and that $\Delta H/D$ can be written as $\Delta H/D = \Delta H/h \cdot h/D$, k_s/h must be a function of Ψ and so \bar{u}/u_* is. Fig. 7 and Fig. 8 are obtained by plotting the experimental data against Ψ , from which we find \bar{u}/u_* decrease and k_s/h increase with the increase of Ψ , contrary to the case of channels or rivers with fixed beds. In the recent measurements at the Hii River and the Kimotsuki River this tendency was clearly observed.²⁾

In the end of this section let us examine the relation between k_s and ΔH . To do this the mean curve of $\Delta H/h$ is written on Fig. 8. Although the scattering of the observed points makes it difficult to draw out a definite conclusion, it is likely to be seen that $k_s/\Delta H < 1$ for small Ψ and > 1 for larger Ψ . In this connexion J. W. Johnson's experiments [8] may be quoted. He laid down the roughness battens of rectangular cross-section with height ΔH on the bed of a flume in regular spacing λ perpendicularly to the direction of flow. In this flume he found out that the maximum

¹⁾ It was shown by Prof. Kurihara [7] that the critical shear velocity $u_{*c}^2/\beta s_s g D$ is a function of $\{(g/980)/(\beta(100\nu)^2 s_s)\}^{1/3} \cdot D$. Here β is a parameter of Mr. Sakai and is related to Kramer's M through the formula $\beta = (2+M)/(1+2M)$. The present value 0.033 is obtained from the somewhat corrected formula of original paper under consideration of the later data.

²⁾ The report will be shortly published.

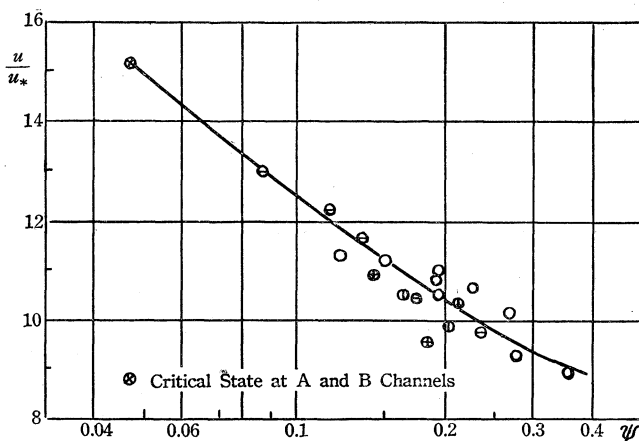


FIG. 7. Mean Velocity in the Channels with Sand Ripples.

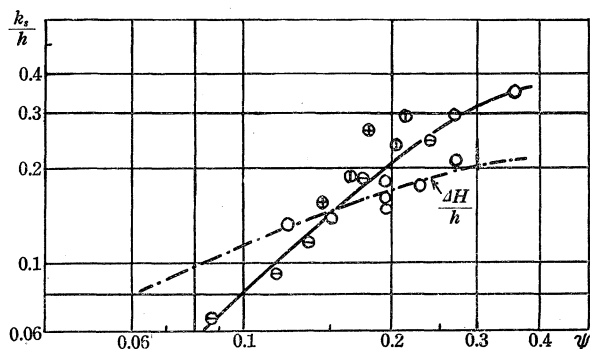


FIG. 8. Equivalent Roughness and its Relation to the Height of Sand Ripples.

relative roughness $k_s/\Delta H \doteq 5$ was attained approximately for $\lambda/\Delta H \doteq 12$. As Fig. 4 (c) shows, $\Delta H/\lambda$ increases with Ψ in our cases and thus the change of $k_s/\Delta H$ with Ψ seems to be closely related to the result of Johnson.

5. The Rate of Sediment Transport. The fact that the rate of sediment transportation is influenced from the sand ripple has been shown recently by H. A. Einstein [9] or one of the present authors [10] and taken into consideration in their formulas. Being the circumstances are so complicated, of course, they could not avoid to depend on rather rough assumptions or purely dimensional analysis. Besides they are based on the results of the flume experiments in laboratories, not on the actual rivers, which must exhibit considerably different features in the scales and natures of the sand ripples. In this section the measured rate of sediment transport is compared with these formulas with some interpretations.

The settling velocity v_s for the mean grain-size of the bed materials in the channels A and B is about 13 cm/sec from Rubey's formula and u_*/v_s was at most 0.67 in the present work. This implies the rôle of suspended load is negligible there, so we shall consider the bed load mainly.

In order to clarify the situation let us summarize later investigations on the bed load of sediment in the followings. The notations q and Φ are defined in p. 244. In 1941 H. A. Einstein [11] related Φ_B/F^{30} to Ψ and A. A. Kalinske [12] expressed q_B/u_*D as a function of Ψ . Here $F = v_s/\sqrt{s_s g D}$ which is to be about 0.8 in his data. Clearly since $q_B/u_*D = \Phi_B \cdot \Psi^{-1/2}$, both of these expressions are essentially equivalent, where Φ_B is considered to be a function of Ψ only. E' and K-curves in Fig. 9 show their results respectively. However, in the presence of sand ripples the other factors than Ψ will play a part, and the sand grains themselves differently behave from the case of the smooth bed. Previously one of the present auther [10] derived the empirical formula

$$\frac{q g s_s}{u_* \left(u_*'^2 - 0.8 \frac{u_* c^2}{\beta} \right)} = 25 \Psi^{4/5} \left(\frac{k_s}{D_{65}} \right)^{-0.44},$$

from the experimental results of G. K. Gilbert, introducing the roughness-parameter k_s/D_{65} . Here u_*' is the critical shear velocity. Or in terms of Φ and Ψ this is rewritten in the form

$$\Phi = 25 \Psi^{1.3} \left(\Psi - \frac{0.8 \Psi c}{\beta} \right) \left(\frac{k_s}{D_{65}} \right)^{-0.44} \quad (7)$$

Einstein on the other hand, published an epoch-making papers on the sediment transport in 1950. He assumed it is the shear velocity u_*' and hydraulic radius R' due to the grain itself that prescribe the flow at the bed, or the flow acting on the grain. According to him, $u_*' = \sqrt{gK'S}$ is given by the following formula:

$$\frac{\bar{u}}{u_*'} = \frac{\bar{u}}{\sqrt{g R' S}} = 5.75 \log \left(\frac{12.2 R'}{D_{65}/x} \right), \quad (8)$$

where x means a correction factor for the departure from the rough region. On this basis, examining the state of turbulence and the mechanism of sediment transport in greater detail, he developed an elaborated theory, which is to be applied to each component of grain-sizes.

For comparison's sake let us consider the most simple case of uniform grains and rough region. Then the bed load function is

$$\Phi_B = \frac{q_B}{\sqrt{s_s g D^3}} = f \left(\frac{u_*'^2}{s_s g D} \right). \quad (9)$$

When the sand ripples are absent, $k_s/D_{65} = 1$ in (7) and $u_*' = u_*$ in (9),

3) The suffix B corresponds to the bed load.

4) Some corrections are made. This formula seems to be applicable for $D \geq 0.3$ mm $\Psi < 1$.

and hence ϕ_n becomes a function of Ψ only from either of (7) or (9). T- and E-curves in Fig. 9 correspond this special case, where we put $0.8\Psi_c/\beta = 0.05$ in (7). The greater difference between them for $\Psi > 0.5$ originates from the suspended load which is taken into account in (7). Both of (7) and (9) show that the more remarkable the sand ripples are, the less ϕ is for equal Ψ . Although in the theories of Einstein (1941) and of Kalinske no special caution has been paid to the sand ripples, it is noticed in Fig. 9 that E'- and K-curves essentially lie below T- and E-curves. This is due to the circumstance that in plotting the experimental data on the plane the influences of the sand ripples are implicitly contained in the values of numerical constants. Next, we shall compare the measured values of the channels A, B and C with E'- and K-curves. In the case of ordinary laboratory work we are used to obtain large Ψ by making the slope S large, whereas in the field work we do this by increasing the depth h . Such a difference produces the different conditions of the beds even for the equal Ψ . For example, in the Gilbert's case, the results of which is served as the fundamental materials of the formula of the sand transport, the sand ripples were already destroying for $\Psi \doteq 0.2$ and disappeared for $\Psi = 0.4 - 0.6$ when the sands of 0.3-0.8 mm diameters were used. If Ψ was increased further there appear the so-called anti-dunes, which go up against the flow. On the contrary in our present case the ripples developed more and more with the increase of Ψ . In the other words the ripples in the tests of large scale are in general more remarkable than those in the experimental flume. This may be the reason why the observed values of ϕ is always below E'- and K-curves for equal Ψ .

To proceed further, T_1 -curve in Fig. 11 is constructed by evaluating the values of k_s/D_{65} graphically from the curves of Fig. 7 and then substituting them in (7). Though (7) is obtained from the experiments of Gilbert, which are in quite different conditions from our test concerning the nature of the ripples, the experimental points in the channels A and B gather fairly near this curve. Alternatively evaluating u_*' through (8) and Fig. 7 and calculating the total load after Einstein's method, we have E_1 -curves in the same plane. The calculated values are considerably lower than the observed ones. In view of the various experimental coefficients contained in his method, the cause of this is not clear, but the followings may still be mentioned: Einstein introduced the coefficient of the pressure reduction ξ , under the assumption that the finer grains lying between the larger ones are protected from the direct action of the flow in the shadow of the stream. And according to him, the sands, of which grain-size is $0.6 > D > 0.3$ mm, can be almost negligible. In our present case, however, the sand ripples act as a sort of the shieving mechanism and we must think the grains which constitute the crests of ripples are exposed to the flow. So that it is natural to suppose that we have overestimated the effect of sheltering after Einstein's schema. E_2 -curve is thus obtained tentatively, neglecting this effect throughly. The accordance with the observed values is greatly improved for $\Psi > 0.15$.

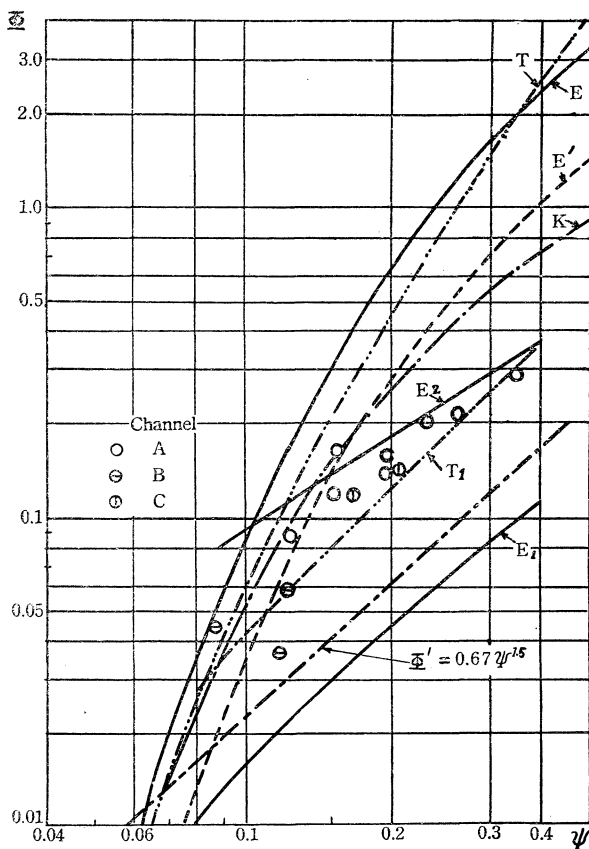


FIG. 9. Comparison of the Observed Data with the Various Formulas.

Finally the advance velocities of the ripples (§3) or the rates of sediment transport in the form of sand ripples are plotted in Fig. 9. The difference between Φ and Φ' is an indication of continuous substitution of constituent grains. We have here about 2.5 as the ratio of Φ and Φ' throughout the tests.

6. Summary and Acknowledgement. In conclusion it becomes clear that the existence of sand ripples largely influences the conditions of the stream and the sediment transport in the channels or rivers. But as these phenomena have wide varieties according to the physical conditions, we have to say that much more extensive studies are needed in order to describe the character of the ripples in terms of the hydraulic conditions of the flow and the bed materials with sufficient generality.

The authors heartily express their thanks to Professors M. Kurihara, K. Shinohara and M. Tamachi of Kyushu University for their helpful guid-

ances and continual encouragements. The acknowledgements are also due to Mr. R. Kawaharada, A. Furuya, H. Kawano and M. Ibusuki for their kind cooperations in the experimental work.

References

- [1] N. Mononobe, Hydraulics. (in Japanese). p. 248.
- [2] M. Kurihara and T. Tsubaki, On Roll Waves in shallow Water flowing in Flat Bottom channel. (in Japanese). Rep. of Res. Inst. for Hydraulic Eng. Kyūshū Univ. vol. 6, No. 1. 1949.
- [3] S. Nagai, Researches on the Movement of the Sand of the River Bed of the Ryoga. (in Japanese). Jour. of Civ. Eng. Soci. of Japan. vol. 27, No. 1. 1941.
- [4] K. Aki and S. Sato, Experimental Research on the Flow characteristics of Rivers with Sand Transport and on the Critical Tractive Force. (in Japanese). Rep. of Res. Inst. of Civ. Eng. vol. 48. 1939.
- [5] H. A. Einstein and N. L. Barbarossa, River channel Roughness. Proc. A.S.C.E. 1951.
- [6] T. Tsubaki and A. Furuya, On the Resistance Law of Rivers with Sand Transport. (in Japanese). Rep. of Res. Inst. for Hydraulic Eng. Kyūshū Univ., vol. 7, No. 4. 1951.
- [7] M. Kurihara and T. Tsubaki, On the Critical Tractive Force. Rep. of Res. Inst. for Hyd. Eng. Kyūshū Univ. vol. 6, No. 2. 1950.
- [8] J. W. Johnson, Rectangular Artificial Roughness in Open channels. Trans. Ame Geophy. Union. 1944.
- [9] H. A. Einstein, The Bed Load Function for Sediment Transportation. Technical Bulletin. No. 1026. U.S. Dept. of Agriculture. 1950.
- [10] T. Tsubaki, On the transportation of Sands in the Open channels. (in Japanese). Rep. Res. Inst. for Hyd. Eng. Kyūshū Univ. vol. 7, No. 4. 1951.
- [11] H. A. Einstein, Formulas for the Transportation of Bed Load, Trans. A.S.C.E. vol. 107. 1942.
- [12] A. A. Kalinske, Movement of Sediment as Bed Load in Rivers. Trans. Ame. Geophy. Union. 1947.

(Received July 30, 1953)